

Adaptive Local Entropy Based Automatic Virus Particle Detection

Hizana M, Anto Kumar R P

P.G Scholar, Dept. of Information & Communication Engineering,
St.Xavier's Catholic College of Engineering, Nagercoil, Tamilnadu, India.
Assistant Professor, Dept. of Information Technology,
St. Xavier's Catholic College of Engineering, Nagercoil, Tamilnadu, India

Abstract

In this project, a fully automatic approach to locate icosahedral virus particles in transmission electron microscopy images is proposed. For segmentation, we present random walker segmentation method to improve the efficiency and accuracy of the segmentation. Firstly, feature information has been employed to combine with the intensity information to measure weights between adjacent nodes (pixels). The parameters have been then adjusted for the two features above to obtain the scale. Secondly, Morphological features help to select the candidates, as the threshold is kept low enough to avoid false negatives. The candidate points are subject to a credibility test based on features extracted from eight radial intensity profiles in each point from a texture image. A candidate is accepted if these features meet the set of acceptance conditions describing the typical intensity profiles of these kinds of particles. When compared with the existing method our propose approach has good performance and high segmentation accuracy.

KEYWORDS — ENTROPY, ICOSAHEDRAL VIRUS, SEGMENTATION, AUTOMATIC SELECTION, ELECTRON MICROSCOPY IMAGES.

I. INTRODUCTION

Manual selection of single particles in images acquired using cryo-electron microscopy (cryoem) will become a significant bottleneck when datasets of a hundred thousand or even a million particles are required for structure determination at near atomic resolution.[1] algorithm development of fully automated particle selection is thus an important research objective in the cryoem field. A number of research groups are making promising new advances in this area. evaluation of algorithms using a standard set of cryoem images is an essential aspect of this algorithm development.

Three approaches remain relevant: the texture-based method, with an interactive training phase to select data windows representative of three categories particle, noise and junk — characterized by 8 features plus an estimate of the particle area.[12] These features enable a linear maximum likelihood discriminate analysis for further classification of other candidate data windows: a supervised classification in a 9-dimensional space of the candidates (located by convolution of the decimated image with a Gaussian of width related to the particle size and a peak search algorithm with specific constraints). The cross-point method developed for spherical virus particles, assumes that there is a constant relation between the intensity levels of the pixels inside a particle and the pixels in the

background, and explores that relation. Post refinement is achieved by correlation with a model particle built as an average of all the particles detected. Icosahedral particles have also been detected by the local average intensity method , an automatic method that locates the initial point candidates comparing the average intensity value in a particle-sized circle with the average in a ring around that circle, and keeping the maxima of that ratio in each square of image with diagonal equivalent to the particle radius; in a second phase, these candidates are evaluated according a set of rules relating the intensities in 8 sectors of the circle and the corresponding sectors in the external ring, reduced to half of the initial thickness. A final pruning limits the possibility of duplicated selection of the same particle in two adjacent squares. In this work, we have developed a two-step multi-frame association finding algorithm which is based on a temporally semi-global formulation as well as combines a spatially global and a spatially local approach. Using this multiframe association finding algorithm we have developed a probabilistic tracking approach based on the Kalman filter. Compared to spatially global approaches, our association finding algorithm can better cope with spurious objects by selecting highly likely associations in the first step and using multi-frame optimization for the unmatched particles in the second step. Key properties of our approach are

multi-frame optimization, verification of associations with past and subsequent positions of the particles, correction of erroneous associations, and robust estimation of the position of particles. Compared to , our approach simultaneously exploits the information from several consecutive time points. Unlike, our approach performs particle linking and detection of clustering and unclustering simultaneously. We have quantitatively evaluated our approach using synthetic as well as real fluorescence microscopy image sequences displaying avian leucosis virus (ALV) particles and performed comparison with previous approaches.

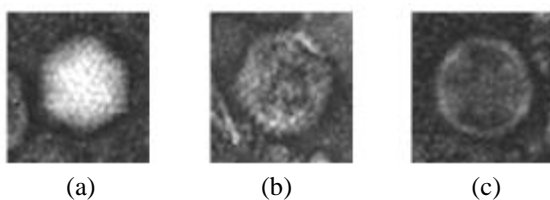


Fig 1: Icosahedral virus particles (a) Capsid intact (b) damaged and (c) completely full of organic and stain materials.

The first processing step for virus particles with icosahedral symmetry is the selection of virus particles from electron micrograph images. Traditionally, the selection of particles has been performed by hand.[9] In addition to being a slow monotonous process prone to human error, fatigue, and subjectivity, this method is also hindered by low image contrast which often makes particles very difficult to identify. This paper describes an automatic particle selection method which detects virus particles in extremely low contrast close to focus images.

Due to the spherical nature of virus particles we have chosen to use template matching [1, 2] for particle selection. While basic template matching is well suited to identifying circular projection images of virus particles, several issues must be addressed in order to provide an accurate and efficient particle selection method. These issues include the choice of a reference image, efficient image processing size, and compensation for the contrast gradients and spatial variation present in these images. We have modified the basic template matching algorithm to compensate for such image artefacts.

Most animal viruses are icosahedral or near-spherical with icosahedral symmetry. Regular icosahedrons is the optimum way of forming a closed shell from identical sub-units. The minimum number of identical capsomers required is twelve, each composed of five identical sub-units. Many viruses, such as rotavirus, have more than twelve capsomers and appear spherical but they retain this symmetry. Capsomers at the apices are surrounded by five other capsomers and are called pentons. Capsomers on the

triangular faces are surrounded by six others and are called hexons. Hexons are in essence flat and pentons, which form the 12 vertices, are curved. The same protein may act as the subunit of both the pentamers and hexamers or they may be composed of different proteins.

II. RELATED WORK

In electron cryo microscopy, projection images are used to determine the three dimensional structures of macromolecular complexes. [1]The first processing step for virus particles with icosahedral symmetry is the selection of virus particles from electron micrograph images. Traditionally, the selection of particles has been performed by hand. In addition to being a slow monotonous process prone to human error, fatigue, and subjectivity. Due to the spherical nature of virus particles we have chosen to use template matching [1, 2] for particle selection. While basic template matching is well suited to identifying circular projection images of virus particles, several issues must be addressed in order to provide an accurate and efficient particle selection method. These issues include the choice of a reference image, efficient image processing size, and compensation for the contrast gradients and spatial variation present in these images. First, the image is divided into small square sub images. Each sub image is then processed individually as follows. For spot-scan and other highly spatially varying images the optional black area correction and Fourier space filtering are performed as pre processing steps.[10] Next, the correlation image is calculated. If black area corrections are being performed the mask is applied to the correlation image to ensure accurate peak selection. The hand selected particle count was used as the true number of particles in the micrographs. These tests have shown that template matching is able to identify virus particles independent of the image defocus value . Particles can be detected on both flood beam and spot-scan images with the same accuracy. On average we have found that 85% of the particles are extracted from a given image.[3] The remaining 15% generally lie near spot-scan edges or ice contamination. The selected particles are very accurately centered. Unfortunately, this method is not sensitive. That is, a large amount of non-particle image areas are also selected. Our tests have shown that as many as 50% of the selected images are not particles. This is due to the inaccuracy of a template in very noisy images, as well as our peak by the template matching method.

Two fundamental concepts of computational geometry, namely, the distance transform and the Voronoi diagram, are used for detection of critical features as well as for accurate location of particles from the images or micrographs.[10] Our approach is fully automatic and has been successfully applied to

detect particles with approximately circular or rectangular shapes (e.g., KLH particles). Particle detection can be enhanced by multiple sets of parameters used in edge detection and/or by anisotropic filtering. In contrast to X-ray diffraction technique, the single particle method does not require formation of crystals. However, the signal-to-noise ratio (SNR) in most cryo-EM images [2] is very low due to various reasons, such that high-resolution single particle analysis often has to rely on averaging of a large number of identical particles. Therefore, locating most, if not all, of the particles in the digitized cryo-EM images is a crucial step in high-resolution single particle reconstruction. Another commonly used approach is based on template-matching, where the template is chosen as a rotationally averaged image of manually picked particles.[8] The template is cross correlated with the entire image and the “peaks” of the resulting cross correlation map are identified as particles. This method, however, may fail for non-spherical particles or for multiple-view particles by the particle picking methods.

The micrograph is the non-Markovian field. The image segmentation step involves an estimation of coupling parameters and the maximum a posterior estimate of the realization of the Markovian field i.e., segmented image. The initial step in three-dimensional structural studies of single particles and viruses after electron micrographs have been digitized is the selection (boxing) of particles images. Traditionally, this task has been accomplished by manual or semi-automatic procedures. The signal-to-noise ratio (SNR), and in general the characterization of the noise in a micrograph, are very important to determine the best technique for automatic particle identification to be used for that micrograph.[4] Noise estimation could help the automatic selection of the parameters of an edge detection algorithm.

Automatic selection of particle projections from a micrograph requires that the results be obtained reasonably fast. Hence, in addition to analysis pertinent to the quality of the solution, report the time required by the algorithm for different size and number of particles in a micrograph. The time devoted to different phases of our algorithm and demonstrates that pre-processing and segmentation account for 97–99% of the computing time. A significant portion of the time is spent in obtaining an optimization for the MRF. This can be overcome if a multi-scale technique is adopted. With a multi-scale technique, a series of images of smaller size, with larger pixel dimensions, are constructed. The optimization starts with the smallest size image, corresponding to the largest scale. The results are propagated to the optimization for the same image but of larger size, at next scale by the markov random field.

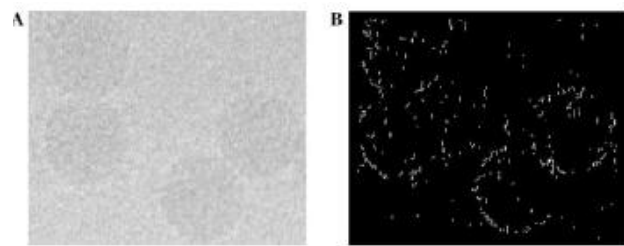


Fig 2: Electron microscopic images of virus particles.

A number of research groups are making promising new advances in this area. Evaluation of algorithms using a standard set of cryoEM images is an essential aspect of this algorithm development. With this goal in mind, a particle selection “bakeoff” was included in the program of the Multidisciplinary Workshop on Automatic Particle Selection for cryoEM. Due to the specific nature of the dataset, the major goal of the bakeoff focuses more on how to compare and contrast the results of different algorithms and less on the performance of individual algorithms.[5] As we know, even for experts, the final set of particles selected from the same set of images may vary from person to person. For this reason, we currently assess the results from different participants by comparing one result against another, measured by the false negative rate (FNR) and false positive rate (FPR) by the manual selection method.

Cell filopodia are segmented and virus particles are detected. Second, the segmentation result is used to discriminate surfing virus particles from other particles. Third, a probabilistic tracking approach based on independent particle filters is used for tracking surfing virus particles. Fourth, the direction and speed of the movement of surfing virus particles towards or away from a cell are determined. Our approach has been applied to synthetic as well as real microscopy image sequences. To quantitatively evaluate the performance, the following measures were calculated. [6] The number of correct trajectories (CT) (i.e., trajectories which start when particles attach to filopodia and finish when they invade cells, and which have no gaps), mostly correct trajectories (MT) (i.e., trajectories which start later than the time point of attachment to filopodia and/or finish before the time point of invasion, which have no gaps, and contain more than 50% of correctly tracked time steps), and mostly lost trajectories (ML) (i.e., trajectories as for MT, but which contain less than or equal to 50% of correctly tracked time steps), as well as the number of trajectory fragments (TF), and the number of false positives (FP) (trajectories of virus particles which do not move along cell by the virus surfing method).

The random walker algorithm is an algorithm for image segmentation. In the first description of the algorithm, a user interactively

labels a small number of pixels with known labels (called seeds), e.g., "object" and "background". The unlabeled pixels are each imagined to release a random walker, and the probability is computed that each pixel's random walker first arrives at a seed bearing each label, i.e., if a user places K seeds, each with a different label, then it is necessary to compute, for each pixel, the probability that a random walker leaving the pixel will first arrive at each seed. This computation may be determined analytically by solving a system of linear equations. After computing these probabilities for each pixel, the pixel is assigned to the label for which it is most likely to send a random walker. The image is modelled as a graph, in which each pixel corresponds to a node which is connected to neighbouring pixels by edges, and the edges are weighted to reflect the similarity between the pixels. Therefore, the random walk occurs on the weighted graph.

The random walker algorithm was initially motivated by labelling a pixel as object/background based on the probability that a random walker dropped at the pixel would first reach an object (foreground) seed or a background seed. Consequently, the random walker algorithm has two different interpretations.

$$rij = \frac{1}{wij}$$

In the first interpretation, each node associated with a background seed, is tied directly to ground while each node associated with an object/foreground seed, is attached.[7] In the second interpretation, labelling a node as object or background by thresholding the random walker probability at 0.5 is equivalent to labelling a node as object or background based on the relative effective conductance between the node and the object or background seeds .

Step 1: Learn the constraint-free optimal projection of the training data, X, e.g. using graph embedding (GE)

$$Wy=\lambda Dy$$

where y is the projection of X in the subspace defined by W. W_{ij} models the intrinsic relationships between samples i and j of the training data, and D is a diagonal matrix with $D_{ii} = \sum_j W_{ij}$. The advantage of GE is that it enables various subspace learning algorithms to be used as classifiers by simply varying W.

Step 2: Determine the classifier weights a such that y and Xa are as similar as possible under the desired constraints:

$$\hat{a} = \min_a \|y + Xa\|^2 + \|\Gamma\|^2$$

If we then transform by augmenting X and y as follows:

$$\tilde{X} = (1 + \alpha)^{-\frac{1}{2}} \begin{pmatrix} X \\ \sqrt{\alpha} \Gamma \end{pmatrix}, \tilde{y} = \begin{pmatrix} y \\ 0 \end{pmatrix}$$

The Application for the random walker segmentation is the Medical Image Segmentation, Image Colorization, Mesh Segmentation and Shadow Elimination.

III. SYSTEM MODEL

A. PRE-PROCESSING

The Pre-Processing is the basic step which is used for the image acquisition method. The pre-processing method includes several methods such as morphology compensation, Wavelet filter, Wiener filter and the Histogram Equalization.

i. Morphology Compensation

The Morphology compensation is used to compensate the irregular background of the image. Morphological Closing after Opening is done in the Morphology Compensation of the image. It is used in the image enhancement and Noise removal. In the sample image, the background illumination is brighter in the center of the image than at the bottom. In this step, the example uses a morphological opening operation to estimate the background illumination. Morphological opening is an erosion followed by a dilation, using the same structuring element for both operations. The opening operation has the effect of removing objects that cannot completely contain the structuring element. For more information about morphological image processing, see Morphological Filtering. The example calls the imopen function to perform the morphological opening operation. Note how the example calls the strel function to create a disk-shaped structuring element with a radius of 15. To remove the rice grains from the image, the structuring element must be sized so that it cannot fit entirely inside a single grain of rice.

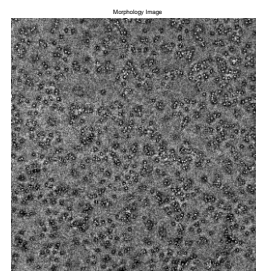


Fig 3: Image with Uniform Background using the Morphology Compensation.

The disk level structuring element is compensated by the top hat morphological method. The top hat meaning is the Erosion and Dilation of the small object.

ii. Wavelet Filter

The Wavelet filter is done by the Daubechies filter. The Wavelet is the wave- like amplitude which is increases and decreases back to zero. It is used for converting the spatial domain to the sub-band domain. It extract the wavelet co-efficient and then apply the quantization. The quantization is a lossy Compression technique achieved by compressing a range of value to a single quantum value. For example, reducing the number of colours required to represent a digital image makes it possible to makes it possible to reduce file size. The unknown region is removed. The wavelet spike filter is used to filter the high value coefficients.

$$x(t) = \sum_{m \in Z} \langle x, \kappa_m, n \rangle \sum_{n \in Z} \kappa_m, n(t)$$

The frequency bands or subspaces (sub-bands) are scaled versions of a subspace at scale 1. This subspace in turn is in most situations generated by the shifts of one generating function ψ in $L^2(\mathbb{R})$, the mother wavelet. For the example of the scale one frequency band [1, 2] this function is used. Wavelet transforms can be used to transform data, then encode the transformed data, resulting in effective compression. The image enhancement and the restoration can be done by the wavelet filter. The filtering can be done by the different methods for the better performance and the high level values at the higher intensities. The frequency and the band width of the images can be found at the zero values which increases and decreases.

Wavelet theory is applicable to several subjects. All wavelet transforms may be considered forms of time-frequency representation for continuous-time (analog) signals and so are related to harmonic. Almost all practically useful discrete wavelet transforms use discrete-time filter banks. These filter banks are called the wavelet and scaling coefficients in wavelets nomenclature. These filter banks may contain either finite impulse response (FIR) or infinite impulse response (IIR) filters. The wavelets forming a continuous wavelet transform (CWT) are subject to the uncertainty principle of Fourier analysis respective sampling theory: Given a signal with some event in it, one cannot assign simultaneously an exact time and frequency response scale to that event. The product of the uncertainties of time and frequency response scale has a lower bound. Thus, in the scale gram of a continuous wavelet transform of this signal, such an event marks an entire region in the time-scale plane, instead of just one point. Also, discrete wavelet bases may be considered in the context of other forms of the uncertainty principle. Wavelet transforms are broadly divided into three classes: continuous, discrete and multi-resolution-based.

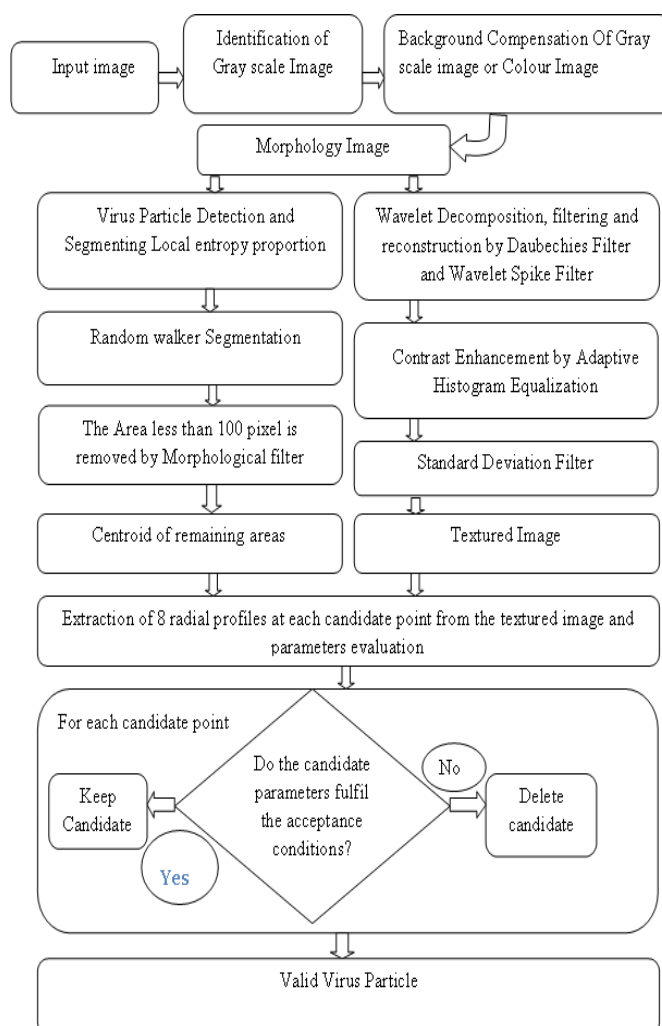


Fig. 4. Diagram for the implementation of the system model.

iii. Wiener Filter

The Wiener filter problem has solutions for three possible cases: one where a non-causal filter is acceptable (requiring an infinite amount of both past and future data), the case where a causal filter is desired (using an infinite amount of past data), and the finite impulse response (FIR) case where a finite amount of past data is used. The first case is simple to solve but is not suited for real-time applications. The Wiener Filter is the combination of the inversion filter and the smoothening filter. The Inverse Filter is used to remove the blur from the images and the smoothening filter is used to remove the noise from the images. Inverse filter restores a blurred image perfectly from an output of a noiseless_linear system. However, in the presence of additive white noise, it does not work well. In this project, how the ratio of spectrum N/H affects on the image restoration_is demonstrated.

$$G = \frac{H(\omega_1, \omega_2) S_{uu}(\omega_1, \omega_2)}{|H(\omega_1, \omega_2)|^2 + S_{uu}(\omega_1, \omega_2) + S_{\eta\eta}(\omega_1, \omega_2)}$$

It is commonly used to denoise audio signals, especially speech, as a preprocessor before speech recognition.

iv. Histogram Equalization

Histogram equalization is a technique for adjusting image intensities to enhance contrast. Let f be a given image represented as a m by n matrix of integer pixel intensities ranging from 0 to $L - 1$. L is the number of possible intensity values, often 256. Let p denote the normalized histogram of f with a bin for each possible intensity. So

$$p_n = \frac{\text{number of pixels with intensities } n}{\text{number of pixels}}$$

The histogram equalized image g will be defined by

$$g_{i,j} = \text{floor}((L - 1) \sum_{n=0}^{f_{i,j}} p_n)$$

where $\text{floor}()$ rounds down to the nearest integer. This is equivalent to transforming the pixel intensities, k , of f by the function. This method usually increases the global contrast of many images, especially when the usable data of the image is represented by close contrast values. Through this adjustment, the intensities can be better distributed on the histogram. This allows for areas of lower local contrast to gain a higher contrast. Histogram equalization accomplishes this by effectively spreading out the most frequent intensity values. The method is useful in images with backgrounds and foregrounds that are both bright or both dark. In particular, the method can lead to better views of bone structure in x-ray images, and to better detail in photographs that are over or under-exposed.

B. RANDOM WALKER SEGMENTATION

The random walker algorithm is an algorithm for image segmentation. In the first description of the algorithm, a user interactively labels a small number of pixels with known labels (called seeds), e.g., "object" and "background". The unlabeled pixels are each imagined to release a random walker, and the probability is computed that each pixel's random walker first arrives at a seed bearing each label, i.e., if a user places K seeds, each with a different label, then it is necessary to compute, for each pixel, the probability that a random walker leaving the pixel will first arrive at each seed. This computation may be determined analytically by solving a system of linear equations. After computing these probabilities for each pixel, the pixel is assigned to the label for which it is most likely to send a random walker. The image is modelled as a graph, in which each pixel corresponds to a node which is connected to neighbouring pixels by edges, and the edges are weighted to reflect the similarity between the pixels. Therefore, the random walk occurs on the weighted graph.

The random walker algorithm was initially motivated by labelling a pixel as object/background based on the probability that a random walker dropped at the pixel would first reach an object (foreground) seed or a background seed. Consequently, the random walker algorithm has two different interpretations.

$$r_{ij} = \frac{1}{w_{ij}}$$

In the first interpretation, each node associated with a background seed, is tied directly to ground while each node associated with an object/foreground seed, is attached. In the second interpretation, labelling a node as object or background by thresholding the random walker probability at 0.5 is equivalent to labelling a node as object or background based on the relative effective conductance between the node and the object or background seeds .

Adaptive sparse classifier:

Step 1: Learn the constraint-free optimal projection of the training data, X , e.g. using graph embedding (GE)

$$Wy = \lambda Dy$$

where y is the projection of X in the subspace defined by W . W_{ij} models the intrinsic relationships between samples i and j of the training data, and D is a diagonal matrix with $D_{ii} = \sum_j W_{ij}$. The advantage of GE is that it enables various subspace learning algorithms to be used as classifiers by simply varying W .

Step 2: Determine the classifier weights a such that y and Xa are as similar as possible under the desired constraints:

$$\hat{a} = \min_a \|y - Xa\|^2 + \|\Gamma a\|^2$$

If we then transform by augmenting X and y as follows:

$$\tilde{X} = (1 + \alpha)^{-\frac{1}{2}} \begin{pmatrix} X \\ \sqrt{\alpha \Gamma} \end{pmatrix}, \tilde{y} = \begin{pmatrix} y \\ 0 \end{pmatrix}$$

The Application for the random walker segmentation is the Medical Image Segmentation, Image Colorization, Mesh Segmentation and Shadow Elimination.

C. FEATURE DESCRIPTORS

The feature Descriptors consist of the textured based features and the region based features and properties. The textured descriptors and the region properties can be calculated by the different formulas such as area, circumferences, ellipticity etc.

i. Textured Features

Image is divided into multiple blocks and the each block is computed by means of standard deviation

formulas. The computed block is then obtained as textured images.

$$\sigma^2 = \frac{1}{N-1} \sum_{i=0}^{N-1} (x_i - \mu)^2$$

The standard deviation of the textured image is found by the above formula. N is the number of the blocks in the images.

ii. Region Properties

Textured segmented image region properties like area, circumference and ellipticity are calculated. The area and the circumference are calculated from the region properties. i.e., when the area is less than 100 pixels, the candidate will select the region by the region property.

D. CANDIDATE SELECTION

The original images with a magnification of 52.000 were digitized at 16 bits and 800 dpi, i.e. about 3900×2800 pixels. The intensive computing of this approach required a re-sampling at 1:3 rate, to reduce the images to an affordable processing time during development. Pre-processing with a wavelet filter, consisting in decomposition (using a Daubechies wavelet of support of order 11) followed by reconstruction with the details of first level suppressed, provided a smooth filter of local spikes. The pre-processed image constitutes the input to the entropy proportion calculation.

$$l_{ep}(i, j) = \frac{n(i, j)}{d(i, j)}$$

The value of the entropy e was computed as the sum

$$e = - \sum [h \log_2(h)]$$

This evaluation was achieved in a texture image built with a standard deviation filter using a 3D structuring element on a pre-processed input image.

E. PERFORMANCE ANALYSIS

The performance analysis was obtained by the ROC(Receiver Operating Characteristics). The ROC can be calculated from the False Positive Rate and the False Negative Rate.

The False Positive Rate (computed as the ratio of erroneous particles of all classes to the total number of particles identified) were below 0.5 ROC. i.e., the percentage of the FPR is 10%

The True Positive Rate is the ratio between the numbers of the missed particles to the total number of the particles identified in the class. The percentage will be 63%

$$TPR = \frac{TP}{TP + FN}$$

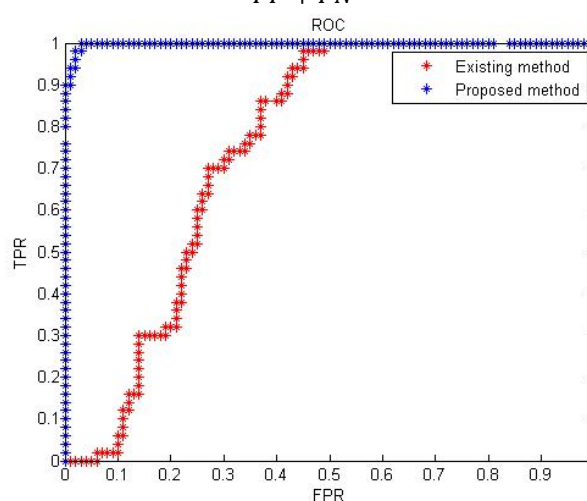
where,

TPR, FPR= True Positive Rate, False Positive Rate

TP, FN= True Positive, False Positive

TN, FN= True Negative, True Negative

$$FPR = \frac{FP}{FP + FN}$$



IV. CONCLUSION AND EXPERIMENTAL RESULTS

The experimental results of the virus particle detection can be performed by many of the method. The Experimental results can be found by the performance by class and particles. When the 100% intact particle is detected, 76% will be permeated and 60% will be damaged. The True Positive Rate of the virus Particles can be obtained by the 60% and the 0.8 of the permeated particles. Since there are many disadvantages in detection of virus automatically, Automatic Virus particle selection was preferred for the identification of the virus more easily and clearly. The initial detection of the particles takes place by automatic segmentation of the entropy-proportion image. The basics for the entropy approach remains valid as long as an area of low entropy can be associated with the object of interest. The detection of the minima in the entropy proportion image can be achieved by many methods, like a peak search algorithm applied to the complement of the image or any other current method; the use of a threshold dependency of the image characteristics aims to simplify this step of the process, and enables the subsequent selection by morphological characteristics of the objects retained.

REFERENCES

- [1] I. Boier Martin, D. C. Marinescu, R. E. Lynch, And T. S. Baker, "Identification Of Spherical Virus Particles In Digitized Images Of Entire Electron Micrographs," *J. Struct. Biol.*, Vol. 120, No. 2, Pp. 146–157, 1997.
- [2] B. Carragher, Y. Zhu, R. M. Glaeser, D. Fellmann, C. Bajaj, M. Bern, F. Mouche, F. De Haas, R. J. Hall, D. J. Kriegman, S. J. Ludtke, S. P. Mallick, P. A. Penczek, A. M.

- Roseman, "Findem—A Fast, Efficient Program For Automatic Selection Of Particles From Electron Micrographs," *J. Struct. Biol.*, Vol. 145, Nos. 1–2, Pp. 91–99, 2004.
- [3] R. M. Glaeser, "Historical Background: Why Is It Important To Improve Automated Particle Selection Methods?" *J. Struct. Biol.*, Vol. 145, Nos. 1–2, Pp. 15–18, 2004.
- [4] C. S. Goldsmith And S. E. Miller, "Modern Uses Of Electron Microscopy For Detection Of Viruses," *Clin. Microbiol. Rev.*, Vol. 22, No. 4, Pp. 552–563, Oct. 2009.
- [5] R. J. Hall And A. Patwardhan, "A Two Step Approach For Semi-Automated Particle Selection From Low Contrast Cryo-Electron Micrographs," *J. Struct. Biol.*, Vol. 145, Nos. 1–2, Pp. 19–28, 2004.
- [6] P. R. Hazelton And H. R. Gelderblom, "Electron Microscopy For Rapid Diagnosis Of Infectious Agents In Emergent Situations," *Emerg. Infect. Diseases*, Vol. 9, No. 3, Pp. 294–303, 2003.
- [7] Z. Huang And P. A. Penczek, "Application Of Template Matching Technique To Particle Detection In Electron Micrographs," *J. Struct. Biol.*, Vol. 145, Nos. 1–2, Pp. 29–40, 2004.
- [8] T. Kivioja, J. Ravantti, A. Verkhovsky, E. Ukkonen, And D. Bamford, "Local Average Intensity-Based Method For Identifying Spherical Particles In Electron Micrographs," *J. Struct. Biol.*, Vol. 131, No. 2, Pp. 126–134, 2000.
- [9] K. R. Lata, P. Penczek, And J. Frank, "Automatic Particle Picking From Electron Micrographs," *Ultramicroscopy*, Vol. 58, Nos. 3–4, Pp. 381–391, 1995.
- [10] W. V. Nicholson And R. M. Glaeser, "Review: Automatic Particle Detection In Electron Microscopy," *J. Struct. Biol.*, Vol. 133, Nos. 2–3, Pp. 90–101, 2001. *Automatic Particle Selection*. (2011, Feb.) [Online]. Available: [Http://Ami.Scripps.Edu/Prtl_Data/](http://Ami.Scripps.Edu/Prtl_Data/)
- [11] T. Ogura And C. Sato, "Automatic Particle Pickup Method Using A Neural Network Has High Accuracy By Applying An Initial Weight Derived From Eigenimages: A New Reference Free Method For Single-Particle Analysis," *J. Struct. Biol.*, Vol. 145, Nos. 1–2, Pp. 63–75, 2004.
- [12] M. Sangreman Proenca, Maria da Conceicao and A.P. Alves de Matos, "Automatic Virus Particle Selection- The Entropy Approach", IEEE Transaction on Image Processing, Vol. 22, Nos 5, May 2013.